A Phase II control chart based on weighted likelihood ratio test for monitoring polynomial profiles

Cailian Yao[a,b], Zhonghua Li [c], Chuan He [d], Jiujun Zhang[a*]

[a]Department of Mathematics, Liaoning University, Shenyang 110036, China

[b]School of Science, Liaoning Shihua University, Fushun 113001, China

[c]School of Statistics and Data Science and LPMC and KLMDASR, Nankai University, Tianjin 300071, China

[d]Department of Mathematics, Northeastern University, Shenyang 118019, China

Abstract

In this paper, a new Phase II control chart based on weighted likelihood ratio test (WLRT) is proposed for monitoring polynomial profiles. The new chart can be easily designed and constructed. Due to the good properties of the likelihood ratio test, computation results show that it provides quite satisfactory performance in various cases, including the detection of the decrease in variance which is very important in many practical applications but may not be well handled by the existing approaches in the literature. Average run length (ARL) comparisons between some other procedures and the new chart are presented. The effect of parameter estimates on WLRT chart is considered. The application of our proposed method is illustrated by a simulation example.

Keywords: Statistical process control (SPC); Polynomial profiles; Weighted likelihood ratio test (WLRT); Average run length (ARL); parameter estimates

1 Introduction

Statistical process control (SPC) plays a very important role in product quality management and improvement. In many SPC applications, the quality of a process or product can be described as a function between a response variable and one or more explanatory variables. This relationship was referred to as profile by Kang and Albin [1]. Many researchers have studied the applications of profiles [2, 3, 4, 5, 6]. The "profile monitoring" methods use statistical methods to check whether such functional relationships are stable or not over the time. The research on profile monitoring in

*Corresponding author, email: zjjly790816@163.com

the SPC field is relatively new in recent years, and the most effective tool for profile monitoring is the control chart. Some researchers have proposed designed methods of control charts for monitoring different profiles in both Phase I and Phase II. The control charts in Phase I are designed to check the statistical stability of the process and to estimate the parameters. However, the control charts in Phase II are adopted to detect parameter changes as quickly as possible.

Early research on profile monitoring mainly assumes that the profile is linear when the process is in control (IC). Various linear profile monitoring charts have been proposed. Kang and Albin [1] introduced two control charts for Phase II monitoring of simple linear profiles. One of these is a multivariate T^2 chart and the other is a combination of an exponentially weighted moving average (EWMA) chart and a range (R) chart. Kim et al. [7] used the centralized x values to ensure the independence of regression parameters, and then detected shifts of regression parameters by three separate EWMA charts. Mahmoud and Woodall [4] suggested a Phase I control chart in combination with F-test method to monitor the error standard deviation and regression parameters. Noorossana and Amiri [8] recommended the combined use of multivariate cumulative sum (MCUSUM) method of Healy [9] and R chart of Kang and Albin [1] to monitor simple linear profiles in Phase II. Woodall et al. [5] gave an overall review on profile monitoring and pointed out the research directions in the future. Change point methods were adopted by Zou et al. [10] and Mahmoud et al. [11] for Phases I and II monitoring with simple linear profile data, respectively. Noorossana and Amiri [12] employed a combined MCUSUM/χ^2 control chart. A new review paper on profile monitoring research was summarized by Woodall [13]. Ghahyazi et al. [14] considered the monitoring methods for linear profiles when the processes are multistage. Linear mixed models were suggested by Jensen et al. [15] to explain the autocorrelation within linear profiles. The monitoring approach was provided by Noorossana et al. [16] when autocorrelation exists in the linear profiles. Zhang et al. [17] used Gaussian process models for monitoring linear profiles with within-profile correlation. The application of nonlinear profiles were introduced by some scholars [18, 19, 20, 21].

A Phase II multivariate EWMA (MEWMA) chart was proposed by Zou et al. [22] to monitor the parameters of general linear profiles. Eyvazian et al. [23] suggested four schemes to monitor multivariate multiple linear regression profiles. Khedmati and Niaki [24] considered a monitoring method for general linear profiles when autocorrelation is presented in Phase II. Zhang et al. [25] suggested an EWMA type chart on the basis of likelihood ratio test (LRT) to monitor simple linear profile parameters. Li et al. [26] used a variable sampling intervals (VSI) EWMA chart to monitor linear profiles. Noorossana et al. [27] provided more details about profile monitoring. Xu et al. [28] proposed a generalized likelihood ratio (GLR) chart for detecting linear profiles. Zhang et al. [29] employed an EWMA chart based on score-test to monitor the changes in linear profiles. In addition, Awad [30] used profile monitoring approach for fault detection of fuel systems. Nie et al.

[31] suggested a method of identifying change-point of nonlinear profiles by data-segmentation. Yang et al. [32] applied dynamic probability control limits to monitor nonparametric profiles. A weighted score test was used by Liu et al. to monitor surgical outcomes [33].

In many practical situations, a profile can be modeled as a polynomial regression profile. Some charts used for monitoring linear and general linear profiles can be modified and used to monitor polynomial profiles. Besides the T^2 chart introduced by Kang and Albin [1], MCUSUM/χ^2 chart proposed by Noorossana and Amiri [12], MEWMA chart suggested by Zou et al. [22], Kazemzadeh et al. [34] suggested a Phase I control chart based on change point. Kazemzadeh et al. [35] proposed a Phase II control chart based on orthogonal polynomial transformation, which is referred to as Ortho chart hereafter. Because three separate EWMA charts and their control limits are needed separately for monitoring parameters, this method is very inconvenient in application for higher order polynomial profiles. In addition, the decrease of variance can not be detected by Ortho chart.

The weighted likelihood ratio test (WLRT) scheme was introduced to monitor the Poisson rates by Zhou et al. [36]. Qi et al. [37] proposed WLRT idea for monitoring generalized linear profiles. Qi et al. [38] also proposed WLRT chart for statistical monitoring of queueing systems. Zhang et al. [39] proposed a weighted-likelihood scheme to monitor censored lifetime data. Song et al. [40] suggested a synthetic chart for monitoring the parameters of a normally distributed process based on the WLRT method. In this paper, we propose a new Phase II control chart to monitor polynomial profiles based on WLRT scheme. The new chart is easily designed and constructed. Some numerical results and comparison have been given. It has been shown that the new chart has an average run length (ARL) performance that is superior to other procedures.

The remainder of this paper is organized as follows. The new WLRT chart for monitoring Phase II polynomial profile is described in Section 2. The control limits and performance of the proposed chart are presented in Section 3. The performance comparisons between our new chart and some other existing charts are given in Section 4. The effect of parameter estimates on WLRT chart is considered in Section 5. The application of our new chart is illustrated by a simulated example in Section 6. Conclusion remarks are given in Section 7.

2 The proposed WLRT scheme

Denote by $\{(x_i, y_{it}),\ i = 1, 2, \cdots, n\}$ the tth random sample collected over time. When the process is in control (IC), the relationship between the response and explanatory variables is assumed to be

$$y_{it} = a_0^{(t)} + a_1^{(t)} x_i + a_2^{(t)} x_i^2 + \cdots + a_m^{(t)} x_i^m + \varepsilon_{it}, i = 1, 2, \cdots, n, t = 1, 2, \cdots, \quad (1)$$

The error terms between profiles $\varepsilon_{it} (i = 1, 2, \cdots, n, t = 1, 2, \cdots)$ are independent and identically distributed as $N(0, \sigma^2)$ and the explanatory variable $x_i, i = 1, 2, \cdots, n$ can be designed to be fixed

from profile to profile.

In order to eliminate the effect of multicollinearity, the explanatory variable x_i can be centralized as $x_i^*, i = 1, 2, \cdots, n$ and the equivalent model of equation (1) can be rewritten as

$$y_{it} = b_0^{(t)} + b_1^{(t)} x_i^* + b_2^{(t)} x_i^{*2} + \cdots + b_m^{(t)} x_i^{*m} + \varepsilon_{it}, i = 1, 2, \cdots, n, t = 1, 2, \cdots, \tag{2}$$

where

$$b_l^{(t)} = \sum_{s=l}^{m} a_s^{(t)} \binom{s}{l} \overline{x}^{s-l}, l = 0, 1, \cdots, m, x_i^* = x_i - \overline{x}, \overline{x} = \frac{1}{n} \sum_{i=1}^{n} x_i, \varepsilon_{it} \sim N(0, \sigma^2) \tag{3}$$

and

$$y_{it} \sim N(b_0^{(t)} + b_1^{(t)} x_i^* + b_2^{(t)} x_i^{*2} + \cdots + b_m^{(t)} x_i^{*m}, \sigma^2). \tag{4}$$

The probability density function of y_{it} is

$$f(y_{it}) = \frac{1}{\sqrt{2\pi}\sigma} \exp\left\{ -\frac{1}{2\sigma^2} (y_{it} - b_0^{(t)} - b_1^{(t)} x_i^* - b_2^{(t)} x_i^{*2} - \cdots - b_m^{(t)} x_i^{*m})^2 \right\}.$$

The parameters $b_0^{(t)}, b_1^{(t)}, b_2^{(t)}, \cdots, b_m^{(t)}$ for the models (2) and (4) are assumed to be known and $\sigma^2 = \sigma_0^2$ when the process is IC. It should be pointed out that at least one of the parameters is changed when the process is out-of-control (OC).

Given a sample $(x_i^*, y_{it}), i = 1, 2, \cdots, n$, consider the following hypothesis test:

$$\begin{aligned} &H_0 : b_0^{(t)} = B_0, b_1^{(t)} = B_1, \cdots, b_m^{(t)} = B_m, \sigma^2 = \sigma_0^2, \\ &H_1 : b_0^{(t)} \neq B_0 \ or \ b_1^{(t)} \neq B_1 \ or \ , \cdots, \ or \ b_m^{(t)} \neq B_m \ or \ \sigma^2 \neq \sigma_0^2. \end{aligned} \tag{5}$$

For convenience, let $\theta = (B_0, B_1, \cdots, B_m, \sigma_0^2)$. The log-likelihood function of response variable y_{ij} can be expressed as:

$$\begin{aligned} l_j(\theta) &= \log \prod_{i=1}^{n} f(y_{ij}) \\ &= \log \left\{ (2\pi\sigma_0^2)^{-\frac{n}{2}} \exp\left[-\frac{1}{2\sigma_0^2} \sum_{i=1}^{n} (y_{ij} - B_0 - B_1 x_i^* - \cdots - B_m x_i^{*m})^2 \right] \right\} \\ &= -\frac{n}{2} (\log 2\pi + \log \sigma_0^2) - \frac{1}{2\sigma_0^2} \sum_{i=1}^{n} (y_{ij} - B_0 - B_1 x_i^* - \cdots - B_m x_i^{*m})^2, \end{aligned} \tag{6}$$

where $i = 1, 2, \cdots, n, j = 1, 2, \cdots$.

For simplicity, ignoring the constant term $\log 2\pi$, a new equation can be obtained:

$$l_j(\theta) = -\frac{1}{2} \left[n \log \sigma_0^2 + \frac{1}{\sigma_0^2} \sum_{i=1}^{n} (y_{ij} - B_0 - B_1 x_i^* - \cdots - B_m x_i^{*m})^2 \right]. \tag{7}$$

The exponentially weighted log-likelihood function is defined on the basis of $l_j(\theta)$:

$$Y_t(\theta, \lambda) = \sum_{j=0}^{t} \omega_{j,\lambda} l_j(\theta), \tag{8}$$

where λ is a smoothing parameter which can be chosen from $(0, 1)$, the weights $\omega_{0,\lambda} = (1 - \lambda)^t, \omega_{j,\lambda} = \lambda(1-\lambda)^{t-j}$, $j = 1, 2, \cdots, t$, and the sum of all the weights is equal to 1. Obviously, all the samples from time point 1 to t are considered to derive $Y_t(\theta, \lambda)$. For $j = 0$, any observation values in the IC sample dataset can be regarded as the values of (x_i, y_{i0}), and the first observation (x_i, y_{i1}) is used in this paper.

The weighted maximum likelihood estimate (WMLE) of θ at time t is defined as

$$\widehat{\theta_t} = arg \max_{\theta} Y_t(\theta, \lambda). \tag{9}$$

As

$$\begin{aligned} Y_t(\theta, \lambda) &= \sum_{j=0}^{t} \omega_{j,\lambda} l_j(\theta) \\ &= \sum_{j=0}^{t} \omega_{j,\lambda} (-\frac{1}{2}) \left[n \log \sigma_0^2 + \frac{1}{\sigma_0^2} \sum_{i=1}^{n} (y_{ij} - B_0 - B_1 x_i^* - \cdots - B_m x_i^{*m})^2 \right] \\ &= -\frac{1}{2} \left[\sum_{j=0}^{t} \omega_{j,\lambda} n \log \sigma_0^2 + \sum_{j=0}^{t} \omega_{j,\lambda} \sum_{i=1}^{n} (y_{ij} - B_0 - B_1 x_i^* - \cdots - B_m x_i^{*m})^2 \frac{1}{\sigma_0^2} \right] \\ &= -\frac{1}{2} \left(Y_{p,t} \log \sigma_0^2 + Y_{c,t} \frac{1}{\sigma_0^2} \right), \end{aligned} \tag{10}$$

where $Y_{p,t} = n \sum_{j=0}^{t} \omega_{j,\lambda} = n, Y_{c,t} = \sum_{j=0}^{t} \omega_{j,\lambda} \sum_{i=1}^{n} (y_{ij} - B_0 - B_1 x_i^* - \cdots - B_m x_i^{*m})^2$.

According to the necessary condition of the extreme value, letting the partial derivative of $Y_t(\theta, \lambda)$ on θ be 0, the $-2\times$logarithm of the WLRT statistic can be obtained as follows (see the Appendix for the detailed derivation process):

$$R_{t,\lambda} = \frac{Y_{c,t}}{\sigma_0^2} + n \log \left(\frac{n\sigma_0^2}{\widehat{Y}_{c,t}} \right) - n. \tag{11}$$

In order to simplify the algorithm, $Y_{c,t}, \widehat{Y}_{c,t}$ can be calculated by the following formulations:

$$Y_{c,t} = (1 - \lambda) Y_{c,t-1} + \lambda \sum_{i=1}^{n} (y_{it} - B_0 - B_1 x_i^* - \cdots - B_m x_i^{*m})^2, \tag{12}$$

$$\widehat{Y}_{c,t} = (1 - \lambda) \widehat{Y}_{c,t-1} + \lambda \sum_{i=1}^{n} (y_{it} - \widehat{B}_0 - \widehat{B}_1 x_i^* - \cdots - \widehat{B}_m x_i^{*m})^2, \tag{13}$$

where $Y_{c,0} = n$, $\widehat{Y}_{c,0} = n$.

The WLRT statistic $R_{t,\lambda}$ can be used as the monitoring statistic. When $R_{t,\lambda}$ exceeds a specified value UCL, i.e. upper control limit , we can say the model parameter $\theta = (B_0, B_1, B_2, \cdots, B_m, \sigma_0^2)$ has changed. The value of UCL is chosen to achieve a specified IC ARL (ARL_0).

3 The performance of WLRT chart

In this section, the performance of the proposed WLRT chart is evaluated. In order to be consistent with other methods, the underlying IC model is considered as follows:

$$\begin{aligned} &y_{it} = A_0 + A_1 x_i + A_2 x_i^2 + \varepsilon_{it} = 3 + 2x_i + x_i^2 + \varepsilon_{it}, \\ &i = 1, 2, \cdots, 10, t = 1, 2, \cdots, \ \varepsilon_{it} \sim N(0, \sigma_0^2). \end{aligned} \tag{14}$$

The fixed explanatory variables are $x_i = 1, 2, \cdots, 10$. In order to eliminate the effect of multicollinearity, all the x_i values are centralized as x_i^* by subtracting the mean of x-values 5.5, then the fixed values are $x_i^* = -4.5(0.5)4.5$ and the transformed model is as follows:

$$\begin{aligned} &y_{it} = B_0 + B_1 x_i^* + B_2 x_i^{*2} + \varepsilon_{it} = \frac{177}{4} + 13x_i^* + x_i^{*2} + \varepsilon_{it}, \\ &i = 1, 2, \cdots, 10, t = 1, 2, \cdots, \ \varepsilon_{it} \sim N(0, \sigma_0^2). \end{aligned} \tag{15}$$

Assume that when the process is OC, the shift form of the parameters are given as follows:

$$A_0' = A_0 + \alpha\sigma_0, \ A_1' = A_1 + \beta\sigma_0, \ A_2' = A_2 + \gamma\sigma_0, \ \sigma' = \delta\sigma_0.$$

Without loss of generality, in our simulation, we assume that $\sigma_0^2 = 1$. Noting that the monitoring statistic $R_{t,\lambda}$ does not have an explicit IC distribution, and there is no direct and simple method to compute the transition matrix, the ARL values are obtained by 50,000 Monte Carlo simulations. The methods have been implemented in a FORTRAN program (available from the authors upon request) that uses the routines "rnnor" to generate Normal random variables.

In order to illustrate the effectiveness of the WLRT chart with different λ, the OC ARL comparisons are shown in Figure 1 (y-axis in log-scale). All of the charts are designed to have the overall IC ARL of 200. The corresponding UCL values are 0.434, 0.975, 2.18, 3.53, 6.69 , respectively, when λ=0.05, 0.1, 0.2, 0.3 and 0.5. From Figure 1, we can see that the proposed WLRT chart performs well on detecting various parameter shifts. In general, a smaller λ leads to a quicker detection of smaller shifts.

[Insert figure 1 about here]

In order to further demonstrate the performance of our new chart, Table 1 presents the OC ARL values when any two parameters shift in the case $\lambda = 0.1$. From Table 1, we can see that the OC ARL of the WLRT chart decreases gradually as the shifts increase. Overall we can see that the WLRT chart can detect any changes in the parameters.

We also conduct some simulations for other choices parameters, including A_0, A_1 A_2 and the degree of polynomials, i,e. m, the preceding findings still hold. Generally speaking, the WLRT chart provides a satisfied performance for various types of shifts. By taking the consideration of its easy design and implementation, we think the WLRT scheme is an alternative in practical applications.

[Insert table 1 about here]

4 Performance comparisons

In this section, we compare our WLRT chart with the other four charts in the literature, called as T^2 chart by Kang and Albin [1], MCUSUM/χ^2 chart by Noorossana and Amiri [12], MEWMA chart by Zou et al. [22] and Ortho chart by Kazemzadeh et al. [35]. Next, we give a brief review of these methods.

First of all, we assume that when the process is IC, the underlying model is given as:

$$y_{it} = A_0 + A_1 x_i + A_2 x_i^2 + \cdots + A_m x_i^m + \varepsilon_{it},\ \varepsilon_{it} \sim N(0, \sigma_0^2), \tag{16}$$

where $i = 1, 2, \cdots, n, t = 1, 2, \cdots$. Let $\widehat{A_t} = (X^T X)^{-1} X^T Y_t$ be the parameter estimator vectors with mean $A = (A_0, A_1, \cdots, A_m)^T$ and covariance matrix $\Sigma = \sigma_0^2 (X^T X)^{-1}$ where X is the sample observation matrix, and Y_t is the tth response vector.

4.1 T^2 chart proposed by Kang and Albin [1]

According to Kang and Albin [1], the T^2 charting statistic is defined as follows:

$$T_t^2 = (\widehat{A_t} - A)^T \Sigma^{-1} (\widehat{A_t} - A). \tag{17}$$

Then T_t^2 follows a central chi-squared distribution with $m+1$ degrees of freedom when the process is IC. The corresponding UCL of T^2 chart is $\chi_\alpha^2(m+1)$, where $\chi_\alpha^2(m+1)$ is the $100(1-\alpha)$ percentile of the chi-squared distribution with $m+1$ degrees of freedom.

4.2 MCUSUM/χ^2 chart proposed by Noorossana and Amiri [12]

According to Noorossana and Amiri [12], the MCUSUM statistic is defined as follows:

$$S_t = \max\{S_{t-1} + a^T (\widehat{A_t} - \mu_G) - 0.5D, 0\}, \tag{18}$$

where $a^T = (\mu_B - \mu_G)^T\Sigma^{-1}/\sqrt{(\mu_B - \mu_G)^T\Sigma^{-1}(\mu_B - \mu_G)}$, $D = \sqrt{(\mu_B - \mu_G)^T\Sigma^{-1}(\mu_B - \mu_G)}$, $\mu_G = A$ is the IC known parameter vector, and μ_B is the OC parameter vector which is related to the minimum shift of parameter. A signal is given when the MCUSUM statistic S_t exceeds a given UCL.

In order to monitor the error variance in combination with the MCUSUM chart, the proposed χ^2 statistic is defined as

$$\chi_t^2 = \frac{1}{\sigma^2}\sum_{i=1}^{n} e_{it}^2, \tag{19}$$

where

$$e_{it} = y_{it} - A_0 - A_1 x_i. \tag{20}$$

The UCL for χ^2 chart can be chosen as $\chi_\alpha^2(n)$, where n is the number of fixed designed points of explanatory variable, and $\chi_\alpha^2(n)$ is the $100(1-\alpha)$ percentile of the chi-squared distribution with n degrees of freedom. This method can be easily used for monitoring polynomial profiles in Phase II. The residuals in this case are calculated as follows:

$$e_{it} = y_{it} - A_0 - A_1 x_i - A_2 x_i^2 - \cdots - A_m x_i^m. \tag{21}$$

4.3 MEWMA chart proposed by Zou et al. [22]

According to Zou et al.[22], they first define

$$Z_t(A) = (\widehat{A_t} - A)/\sigma_0 \tag{22}$$

and

$$Z_t(\sigma_0) = \Phi^{-1}\{F((n-m)\widehat{\sigma}_t^2/\sigma_0^2; n-m)\}, \tag{23}$$

where $\widehat{\sigma}_t^2 = \frac{1}{n-m}(Y_t - X\widehat{A_t})^T(Y_t - X\widehat{A_t})$, $\Phi^{-1}(\cdot)$ is the inverse of the standard cumulative distribution function, and $F(\cdot; v)$ is the chi-squared distribution function with v degrees of freedom. Denote Z_t by $(Z_t(A)^T, Z_t(\sigma_0))^T$. When the process is IC, the $m+1$-dimensional random vector Z_t is distributed as multivariate normal distribution $N_{m+1}(0, \Sigma_Z)$, where 0 and $\Sigma_Z = \begin{pmatrix} (X^TX)^{-1} & 0 \\ 0 & 1 \end{pmatrix}$ are the mean vector and covariance matrix, respectively.

The EWMA charting statistic is defined as

$$W_t = \lambda Z_t + (1-\lambda)W_{t-1}, t = 1, 2, \cdots, \tag{24}$$

with the starting vector value W_0. The MEWMA chart signals when

$$U_t = W_t^T\Sigma_Z^{-1}W_t > L_U\frac{\lambda}{2-\lambda}, \tag{25}$$

where $L_U > 0$ is a control limit parameter and can be chosen by simulation to achieve a specified ARL_0.

4.4 Ortho chart proposed by Kazemzadeh et al. [35]

According to Kazemzadeh et al. [35], under IC situation, the transformed model is as follows:

$$y_{it} = B_0P_0(x_i) + B_1P_1(x_i) + B_2P_2(x_i) + \cdots + B_mP_m(x_i) + \varepsilon_{it},\ \varepsilon_{it} \sim N(0, \sigma_0^2), \tag{26}$$

where $i = 1, 2, \cdots, n, t = 1, 2, \cdots, P_0(x_i), P_1(x_i), \cdots, P_m(x_i)$ are orthogonal polynomials defined such that $\sum_{i=1}^{n} P_r(x_i)P_s(x_i) = 0,\ r \neq s,\ r, s = 0, 1, \cdots, m.\ P_0(x_i) = 1$, and $B_0, B_1, \cdots, B_m$ are orthogonal regression parameters.

The least squares estimators of B_l in each profile are computed by

$$\widehat{B}_{lt} = \frac{\sum_{i=1}^{n} P_l(x_i)y_{it}}{\sum_{i=1}^{n} P_l^2(x_i)}, t = 1, 2, \cdots, l = 1, 2, \cdots, m. \tag{27}$$

Then they use univariate EWMA charts to monitor the parameters of regression model separately.

In order to monitor the error variance σ_0^2, e_{it} and MSE_t are defined as follows:

$$e_{it} = y_{it} - B_0P_0(x_i) - B_1P_1(x_i) - \cdots - B_mP_m(x_i), i = 1, 2, \cdots, n, t = 1, 2, \cdots, \tag{28}$$

$$MSE_t = \frac{1}{n}\sum_{i=1}^{n} e_{it}^2, \tag{29}$$

where $E(MSE_t) = 1$, $Var(MSE_t) = \frac{2\sigma_0^4}{n}$. Then, the EWMA statistics are defined as follows, respectively:

$$EWMA_l(t) = \lambda\widehat{B}_{lt} + (1 - \lambda)EWMA_l(t - 1), \tag{30}$$

$$EWMA_E(t) = \max\{\lambda(MSE_t - 1) + (1 - \lambda)EWMA_E(t - 1), 0\} \tag{31}$$

with the starting values $EWMA_l(0) = B_l$, $EWMA_E(0) = 0$, where $t = 1, 2, \cdots, l = 1, 2, \cdots, m$.

The control limits for $EWMA_l$ in equation (30) and $EWMA_E$ in equation (31) are calculated as follows, respectively:

$$UCL = B_l + K_l\sqrt{\frac{\lambda}{2 - \lambda} \cdot \frac{\sigma_0^2}{\sum_{i=1}^{n} P_l^2(x_i)}}, \tag{32}$$

$$LCL = B_l - K_l\sqrt{\frac{\lambda}{2 - \lambda} \cdot \frac{\sigma_0^2}{\sum_{i=1}^{n} P_l^2(x_i)}}, \tag{33}$$

$$UCL = L_E \sqrt{\frac{\lambda}{2-\lambda} \cdot \frac{2\sigma_0^4}{n}}, \tag{34}$$

where regression multiplier $K_l > 0$ and error multiplier $L_E > 0$ are obtained in order to achieve a specified ARL_0.

4.5 Simulation comparisons

In this section, the WLRT chart is compared with four charts mentioned above in terms of ARL. The control limits or the corresponding design parameters of the above five charts are obtained by simulation. Both the T^2 chart and the MEWMA chart are single chart schemes to monitor the model parameters and error variance, while the MCUSUM/χ^2 chart and Ortho chart are combined control chart schemes.

In order to be consistent with Kazemzadeh et al. [35], we consider the IC model defined by equation (14). The control limits and the corresponding design parameters are presented in Table 2 when $ARL_0 = 200$ and $\lambda = 0.1$. In the MCUSUM/χ^2 chart, we use two one-sided charts for a fair comparison, and we set the OC vectors values equal to (3.1, 2.025, 1.01) and (2.9, 1.975, 0.99), respectively. The control limits for these two one-sided charts (named as MCUSUM_1 and MCUSUM_2) are 6.25 and the control limit for the χ^2 chart is 28.2. Note that this choice of control limits makes the single chart IC ARL approximately 600, and when the combined charts used, the IC ARL approximately 200. Numerical computations based on 50,000 runs are used to determine ARL values and the shift form of parameters considered are the same as that of Kazemzadeh et al. [35].

[Insert table 2 about here]

It should be pointed out that Kazemzadeh et al. [35] only considered the upward shift of error variance and did not consider the downward shift. However, it is also important for monitoring the decrease of variance in practice, because the decrease of variance means enhancement of product quality and improvement. To this end, we also consider the decrease of variance in this paper. The comparison results of OC ARL for detecting any single shift in A_0, A_1, A_2, and σ_0 are presented in Table 3. In addition, simultaneous parameter changes are also considered. In order to save space, the OC ARL values for detecting parameters shift simultaneously are summarized in Table 4-6, as representative examples for illustration (Other kinds of shift results are available from the authors upon request).

[Insert table 3 about here]

[Insert table 4 about here]

[Insert table 5 about here]

[Insert table 6 about here]

According to Tables 3-6, we can draw the following conclusions:

- When the intercept A_0 is changed to $A_0 + \alpha\sigma_0$, the T^2 chart performs worst among all charts. The other four charts perform roughly the same. When $\alpha < 0.25$, the MCUSUM/χ^2 chart performs best, but for several larger shifts ($\alpha \geq 0.25$), the Ortho chart performs best.

- When the second parameter A_1 is changed from A_1 to $A_1 + \beta\sigma_0$, the performance of the Ortho chart and our WLRT chart is similar and both of them perform much better than the other three charts. Our WLRT chart performs best for smaller shifts ($\beta < 0.03$), while the Ortho chart performs a little better than our WLRT chart for moderate shifts ($0.03 < \beta < 0.12$). They have the same performance for larger shifts ($\beta > 0.12$).

- When the third parameter A_2 is changed from A_2 to $A_2 + \gamma\sigma_0$, our WLRT chart performs best in most cases. The Ortho chart performs nearly the same as our WLRT chart for detecting medium and large shifts. The T^2 chart does not perform well in this situation as well, and the OC ARL is nearly 200 for smaller shifts, that is to say the T^2 chart can not detect smaller shifts of parameter A_2. The MEWMA chart and the MCUSUM/χ^2 chart have similar performance.

- When the error standard deviation σ_0 is changed to $\delta\sigma_0$, both upward shift and downward shift of σ_0 are considered. First, in detecting the upward shift of σ_0, the Ortho chart performs best for small and medium shift ($1 < \delta < 1.7$), and our WLRT chart has better performance than the other three charts when $\delta > 1.45$. Second, in detecting the downward shift of σ, our WLRT chart performs best for small and medium shift ($0.65 < \delta < 0.95$), and the MEWMA chart performs best for larger shifts ($\delta < 0.65$). Note that our WLRT chart and MEWMA chart are ARL unbiased, but the other three charts are ARL biased, that is OC ARL is even larger than 200. Yang and Arnold [41] found that the ARL biased control chart would take longer time to detect shifts in the parameter than to trigger a false alarm. So the detection capability of ARL unbiased WLRT chart and MEWMA chart are better than the other three charts.

- When A_0 and A_2 are changed to $A_0 + \alpha\sigma_0$ and $A_2 + \gamma\sigma_0$ simultaneously, the T^2 chart performs worst in all the charts. The Ortho chart performs best for medium and large shifts of A_0, and our WLRT chart has better performance than the other three charts for small shift of A_0 in the case of $\gamma \leq 0.01$. With the increase of γ values, our WLRT chart performs best in the case of $\gamma > 0.01$.

- When A_0, A_1 and A_2 are changed to $A_0 + \alpha\sigma_0$, $A_1 + \beta\sigma_0$ and $A_2 + \gamma\sigma_0$ simultaneously, $\alpha = 0.025$ is taken for example. The T^2 chart performs worst in all the charts. Our WLRT chart and the Ortho chart perform roughly the same, they are the best for all the shifts. For all the γ values, the performance of the MCUSUM/χ^2 chart is better than the MEWMA chart's for $\beta \geq 0.005$. But when $\beta < 0.005$, the MEWMA chart performs a little better than the MCUSUM/χ^2 chart.

- When A_0, A_1, A_2 and σ_0 are changed to $A_0+\alpha\sigma_0$, $A_1+\beta\sigma_0$, $A_2+\gamma\sigma_0$ and $\delta\sigma_0$ simultaneously, $\alpha = 0.025$ and $\beta = 0.005$ is taken for example. The T^2 chart also performs worst in all the charts. Our WLRT chart and the Ortho chart still perform nearly the same, they are also the best for all the shifts. For all the γ values, the performance of the MCUSUM/χ^2 chart is better than the MEWMA chart's for $\delta \geq 1.4$. But when $\delta < 1.4$, the MEWMA chart performs just a little better than the MCUSUM/χ^2 chart.

From the comparison results we can see that our new method performs better than the other methods in small to medium shifts. However, we also observe that no chart performs uniformly better than the other charts. To this end, Han and Tsung [42] proposed using relative mean index (RMI) value to evaluate the overall performance of the charts over a range of shifts. The RMI value of a given control chart is calculated by

$$RMI = \frac{1}{N}\sum_{l=1}^{N}\frac{ARL_{\delta_l} - MARL_{\delta_l}}{MARL_{\delta_l}}, \tag{35}$$

where N is the total number of parameter shifts considered. When a parameter shift δ_l is considered to be detected, ARL_{δ_l} and $MARL_{\delta_l}$ represent the OC ARL of the specified control chart and the smallest OC ARL of all the control charts to be compared, respectively. The smaller the RMI value is, the better the overall performance of the control chart will be. The RMI values of each control chart are computed according to the OC ARL values in Table 3, Table 4, Table 5, and Table 6, respectively. Note that, $N = 65$ and 60 are considered in Table 3 and Table 4-6 respectively. In order to save space, only a small part of shifts are presented in the Tables. The notation "*" in Table 3 means the corresponding OC ARL values are larger than 1000 and the corresponding ARL_{δ_l} value is taken as 1000 in stead.

According to Table 3, the RMI results are 33.07, 1.51, 30.85, 35.64, 0.18 for the MCUSUM/χ^2, MEWMA, Ortho, T^2 and WLRT charts, respectively. For these charts, the corresponding RMI values for Table 4 are 1.96, 2.37, 0.00, 8.29, 0.05, the RMI values for Table 5 are 3.88, 4.17, 0.00 12.36, 0.01, the RMI values for Table 6 are 1.67, 1.86, 0.02, 3.63, 0.14, respectively. From the RMI values we can see that the WLRT chart has the best overall performance when only a single parameter shifts. However, when more than two parameters shift simultaneously, the Ortho chart

has the smallest RMI value and then the WLRT chart, respectively, but the difference is almost negligible.

5 The effect of parameter estimates on WLRT control chart

In the above WLRT control chart, the parameters of model (14) are assumed to be known as $A_0 = 3, A_1 = 2, A_2 = 1, \sigma^2 = 1$. But in many practical applications, the model parameters are unknown, the IC Phase I sample data are needed to estimate the model parameters. In this section, we study the effect of parameter estimates on our WLRT chart.

For the model

$$y_{it} = A_0 + A_1 x_i + A_2 x_i^2 + \varepsilon_{it},\ \varepsilon_{it} \sim N(0, \sigma^2),\ i = 1, 2, \cdots, n,\ t = 1, 2, \cdots,$$

the least square estimates of parameters A_0, A_1 and A_2 for sample t are

$$\begin{pmatrix} \widehat{A}_{0t} \\ \widehat{A}_{1t} \\ \widehat{A}_{2t} \end{pmatrix} = (X^T X)^{-1} X^T Y_t.$$

where

$$X = \begin{pmatrix} 1 & x_1 & x_1^2 \\ 1 & x_2 & x_2^2 \\ \vdots & \vdots & \vdots \\ 1 & x_n & x_n^2 \end{pmatrix}, Y_t = \begin{pmatrix} y_{1t} \\ y_{2t} \\ \vdots \\ y_{nt} \end{pmatrix}.$$

The variance σ^2 of ε_{it} is estimated by the tth mean squared error MSE_t, where

$$MSE_t = \frac{SSE_t}{(n-3)},$$

$SSE_t = \sum_{i=1}^{n} e_{it}^2$ is the residual sum of squares, and $e_{it} = y_{it} - \widehat{A}_{0t} - \widehat{A}_{1t} x_i - \widehat{A}_{2t} x_i^2,\ i = 1, 2, \cdots, n$.

When the parameters of model (14) are unknown, k groups IC Phase I samples are needed to estimate the model parameters. Usually the averages of $\widehat{A}_{0t}$, $\widehat{A}_{1t}$, $\widehat{A}_{2t}$, and MSE_t are considered as the parameter estimates of $A_0,\ A_1,\ A_2,\ \sigma^2$, respectively, i.e.

$$\widehat{A}_0 = \frac{1}{k}\sum_{t=1}^{k} \widehat{A}_{0t},\ \widehat{A}_1 = \frac{1}{k}\sum_{t=1}^{k} \widehat{A}_{1t},\ \widehat{A}_2 = \frac{1}{k}\sum_{t=1}^{k} \widehat{A}_{2t},\ \widehat{\sigma}^2 = MSE = \frac{1}{k}\sum_{t=1}^{k} MSE_t.$$

Without loss of generality, the underlying IC model (14) $y_{it} = 3 + 2x_i + x_i^2 + \varepsilon_{it},\ i = 1, 2, \cdots, n,\ t = 1, 2, \cdots$ is considered, where the $\varepsilon_{it} \sim N(0, 1)$. The run length performance of WLRT control chart with estimated parameters depends on the values of k, n, and λ. For simplicity,

we only consider the case of $n = 10$ in our simulation study, and $x_i = 1, 2, 3, 4, 5, 6, 7, 8, 9, 10$ are chosen so that $\overline{x} = 0$. The five values of k (10, 30, 50, 70, 100) and three values of λ (0.05, 0.10, 0.20) are considered. The IC ARL and SDRL values of WLRT control chart with estimated parameters for different values of k and λ are given in Table 7. From Table 7 we can see that the IC performance of WLRT control chart when estimated parameters are used in designing the control chart statistics is strongly affected if we use the corresponding upper control limits designed based on known parameters. This serious effect is caused by ignoring the variability added by estimating the unknown parameters, this will lead to substantial increase of false alarms as shown in Table 7.

[Insert Table 7 about here]

In order to achieve a desired in control ARL as in the case of model parameters are known, many authors have recommended that the number of Phase I samples m should be increased to an appropriate level to reduce the effect of parameter estimates. So we give the sufficient number of IC Phase I samples needed to produce an IC ARL of 200 for different values of the smoothing parameter λ as follows: $\lambda = 0.05,\ k = 350$, $\lambda = 0.10,\ k = 120$, $\lambda = 0.20,\ k = 100$. The results show that a larger number of Phase I samples is required when smaller λ is used.

In order to achieve the desired IC ARL but without waiting a long time to obtain the IC Phase I sample data, we can use the corrected control limits for different λ and k values. The corrected control limits with estimated parameters are given in Table 8 by simulation. From Table 8, we can obtain that all the corrected control limits are more than the control limits with known parameters.

[Insert Table 8 about here]

So in practical applications, we have two choices to achieve the desired IC ARL when the parameters are estimated. First we can choose appropriate number of IC Phase I samples for different λ. Second we can use the corrected control limits for different λ and k values.

6 An illustrative example

In this section, we demonstrate the application of the proposed WLRT chart by a simulated example. The IC model is the same as equation (14) and $\sigma_0^2 = 1$. First, 20 groups of IC sample data are generated, and then a shift of intercept A_0 is artificially added on the IC model. When the process is OC, it is assumed that the intercept A_0 is shifted from 3 to 3.5, then 20 OC profiles are generated through Monte Carlo simulation. In order to save space, the simulated data are not presented in the paper but available from the authors.

We use this simulated dataset to illustrate the efficiency of the control charts mentioned above. The design parameters of all charts are the same as in Table 2. The charting statistic values are

calculated, and they are shown as plot (a)-(h) in Figure 2. From Figure 2 we can see that the WLRT chart and the MEWMA chart first signal at the 16th and 24th sample respectively, and all the charting statistic values are above the corresponding UCLs after the first signal occurs. The T^2 chart only signals at sample number 18 and 21. In the MCUSUM/χ^2 chart, two MCUSUM statistic values exceed the UCL line for the first time from sample number 22 and 14 respectively. The χ^2 chart never gives a signal. In the Ortho chart, all the $EWMA_1$ statistic values after sample 22 exceed the UCL, except for sample 23, and only the $EWMA_E$ statistic value of sample 22 is above the UCL. Both the $EWMA_2$ and $EWMA_3$ statistic values are in the corresponding control limit intervals. This shows that our WLRT chart is quite a useful alternative tool for practitioners by taking into account its performance of detecting various shifts.

[Insert figure 2 about here]

7 Conclusion remarks

A new Phase II WLRT chart is proposed for monitoring polynomial profiles. The new chart is easily designed and more competitive than the other existing charts in terms of ARL, especially for detecting the decrease of variance. The introduced WLRT chart is a synthetic chart, so it is unable to determine which parameter or parameters have been changed when the WLRT control chart signals. There have been some testing methods for diagnosing simple linear profiles in the literature. For example, Hawkins and Zamba [43] proposed two-sided F test and asymptotic t test. These methods can be applied in diagnosing polynomial profiles.

Acknowledgements

The authors are grateful to the editor and the anonymous referee for their valuable comments that have greatly improved this paper.

Disclosure statement

No potential conflict of interest was reported by the authors.

Funding

This paper is supported by the National Natural Science Foundation of China Grants 11571191 and 11431006, Tianjin science and technology commission Grant 17YFZCSF01280. This paper

is also sponsored by “Liaoning BaiQianWan Talents Program”, the Science and Research Project of Liaoning Educational Department of China No. LSNQN201912.

Appendix

The derivation of equation (11):

As

$$\begin{aligned} Y_t(\theta,\lambda) &= \sum_{j=0}^{t} \omega_{j,\lambda} l_j(\theta) \\ &= -\frac{1}{2}\left(Y_{p,t}\log\sigma_0^2 + Y_{c,t}\frac{1}{\sigma_0^2} \right), \end{aligned}$$

where $Y_{p,t} = n\sum\limits_{j=0}^{t}\omega_{j,\lambda} = n, Y_{c,t} = \sum\limits_{j=0}^{t}\omega_{j,\lambda}\sum\limits_{i=1}^{n}(y_{ij} - B_0 - B_1x_i^* - \cdots - B_mx_i^{*m})^2$.

Taking a partial derivative of $Y_t(\theta,\lambda)$ on θ , and letting the values of the partial derivative be 0, we can obtain

$$\begin{cases} \dfrac{\partial Y_t(\theta,\lambda)}{\partial\sigma_0^2} = -\dfrac{1}{2}\left[n\dfrac{1}{\sigma_0^2} - Y_{c,t}\dfrac{1}{(\sigma_0^2)^2} \right] = 0 \\ \dfrac{\partial Y_t(\theta,\lambda)}{\partial B_0} = \dfrac{1}{2\sigma_0^2}\sum\limits_{j=0}^{t}\omega_{j,\lambda}\cdot 2\sum\limits_{i=1}^{n}(y_{ij} - B_0 - B_1x_i^* - \cdots - B_mx_i^{*m}) = 0 \\ \dfrac{\partial Y_t(\theta,\lambda)}{\partial B_1} = \dfrac{1}{2\sigma_0^2}\sum\limits_{j=0}^{t}\omega_{j,\lambda}\cdot 2\sum\limits_{i=1}^{n}(y_{ij} - B_0 - B_1x_i^* - \cdots - B_mx_i^{*m})x_i^* = 0 \\ \dfrac{\partial Y_t(\theta,\lambda)}{\partial B_2} = \dfrac{1}{2\sigma_0^2}\sum\limits_{j=0}^{t}\omega_{j,\lambda}\cdot 2\sum\limits_{i=1}^{n}(y_{ij} - B_0 - B_1x_i^* - \cdots - B_mx_i^{*m})x_i^{*2} = 0 \\ \qquad\qquad \cdots\cdots\cdots\cdots\cdots\cdots\cdots\cdots\cdots\cdots\cdots\cdots\cdots\cdots\cdots\cdots \\ \dfrac{\partial Y_t(\theta,\lambda)}{\partial B_m} = \dfrac{1}{2\sigma_0^2}\sum\limits_{j=0}^{t}\omega_{j,\lambda}\cdot 2\sum\limits_{i=1}^{n}(y_{ij} - B_0 - B_1x_i^* - \cdots - B_mx_i^{*m})x_i^{*m} = 0. \end{cases}$$

Then

$$\sigma_0^2 = \frac{1}{n}Y_{c,t} = \frac{1}{n}\sum_{j=0}^{t}\omega_{j,\lambda}\sum_{i=1}^{n}(y_{ij} - B_0 - B_1x_i^* - \cdots - B_mx_i^{*m})^2,$$

and

$$\begin{cases} nB_0 + \sum_{i=1}^{n} x_i^* B_1 + \sum_{i=1}^{n} x_i^{*2} B_2 + \cdots + \sum_{i=1}^{n} x_i^{*m} B_m = \sum_{j=0}^{t} \omega_{j,\lambda} \sum_{i=1}^{n} y_{ij} \\ \sum_{i=1}^{n} x_i^* B_0 + \sum_{i=1}^{n} x_i^{*2} B_1 + \sum_{i=1}^{n} x_i^{*3} B_2 + \cdots + \sum_{i=1}^{n} x_i^{*m+1} B_m = \sum_{j=0}^{t} \omega_{j,\lambda} \sum_{i=1}^{n} y_{ij} x_i^* \\ \cdots\cdots\cdots\cdots\cdots\cdots\cdots\cdots\cdots\cdots\cdots\cdots\cdots\cdots\cdots\cdots\cdots\cdots\cdots\cdots\cdots\cdots \\ \sum_{i=1}^{n} x_i^{*m} B_0 + \sum_{i=1}^{n} x_i^{*m+1} B_1 + \sum_{i=1}^{n} x_i^{*m+2} B_2 + \cdots + \sum_{i=1}^{n} x_i^{*2m} B_m = \sum_{j=0}^{t} \omega_{j,\lambda} \sum_{i=1}^{n} y_{ij} x_i^{*m}. \end{cases}$$

Let A be the coefficient matrix of the above non-homogeneous linear equations, i.e.,

$$A = \begin{pmatrix} n & \sum_{i=1}^{n} x_i^* & \sum_{i=1}^{n} x_i^{*2} & \cdots & \sum_{i=1}^{n} x_i^{*m} \\ \sum_{i=1}^{n} x_i^* & \sum_{i=1}^{n} x_i^{*2} & \sum_{i=1}^{n} x_i^{*3} & \cdots & \sum_{i=1}^{n} x_i^{*m+1} \\ \vdots & \vdots & \vdots & \ddots & \vdots \\ \sum_{i=1}^{n} x_i^{*m} & \sum_{i=1}^{n} x_i^{*m+1} & \sum_{i=1}^{n} x_i^{*m+2} & \cdots & \sum_{i=1}^{n} x_i^{*2m} \end{pmatrix}.$$

Then, according to Cramer's rule, the WMLE of $\widehat{B}_0, \widehat{B}_1, \cdots, \widehat{B}_m,$ can be described as follows:

$$\widehat{B}_0 = \frac{\begin{vmatrix} \sum_{j=0}^{t} \omega_{j,\lambda} \sum_{i=1}^{n} y_{ij} & \sum_{i=1}^{n} x_i^* & \sum_{i=1}^{n} x_i^{*2} & \cdots & \sum_{i=1}^{n} x_i^{*m} \\ \sum_{j=0}^{t} \omega_{j,\lambda} \sum_{i=1}^{n} y_{ij} x_i^* & \sum_{i=1}^{n} x_i^{*2} & \sum_{i=1}^{n} x_i^{*3} & \cdots & \sum_{i=1}^{n} x_i^{*m+1} \\ \vdots & \vdots & \vdots & \ddots & \vdots \\ \sum_{j=0}^{t} \omega_{j,\lambda} \sum_{i=1}^{n} y_{ij} x_i^{*m} & \sum_{i=1}^{n} x_i^{*m+1} & \sum_{i=1}^{n} x_i^{*m+2} & \cdots & \sum_{i=1}^{n} x_i^{*2m} \end{vmatrix}}{|A|},$$

$$\widehat{B}_1 = \frac{\begin{vmatrix} n & \sum_{j=0}^{t} \omega_{j,\lambda} \sum_{i=1}^{n} y_{ij} & \sum_{i=1}^{n} x_i^{*2} & \cdots & \sum_{i=1}^{n} x_i^{*m} \\ \sum_{i=1}^{n} x_i^* & \sum_{j=0}^{t} \omega_{j,\lambda} \sum_{i=1}^{n} y_{ij} x_i^* & \sum_{i=1}^{n} x_i^{*3} & \cdots & \sum_{i=1}^{n} x_i^{*m+1} \\ \vdots & \vdots & \vdots & \ddots & \vdots \\ \sum_{i=1}^{n} x_i^{*m} & \sum_{j=0}^{t} \omega_{j,\lambda} \sum_{i=1}^{n} y_{ij} x_i^{*m} & \sum_{i=1}^{n} x_i^{*m+2} & \cdots & \sum_{i=1}^{n} x_i^{*2m} \end{vmatrix}}{|A|},$$

$\cdots$

$$\widehat{B}_m = \frac{\begin{vmatrix} n & \sum_{i=1}^{n} x_i^* & \sum_{i=1}^{n} x_i^{*2} & \cdots & \sum_{j=0}^{t} \omega_{j,\lambda} \sum_{i=1}^{n} y_{ij} \\ \sum_{i=1}^{n} x_i^* & \sum_{i=1}^{n} x_i^{*2} & \sum_{i=1}^{n} x_i^{*3} & \cdots & \sum_{j=0}^{t} \omega_{j,\lambda} \sum_{i=1}^{n} y_{ij} x_i^* \\ \vdots & \vdots & \vdots & \ddots & \vdots \\ \sum_{i=1}^{n} x_i^{*m} & \sum_{i=1}^{n} x_i^{*m+1} & \sum_{i=1}^{n} x_i^{*m+2} & \cdots & \sum_{j=0}^{t} \omega_{j,\lambda} \sum_{i=1}^{n} y_{ij} x_i^{*m} \end{vmatrix}}{|A|}.$$

The WMLE of $\widehat{\sigma}_0^2$ can be obtained as

$$\widehat{\sigma}_0^2 = \frac{1}{n}\widehat{Y}_{c,t} = \frac{1}{n}\sum_{j=0}^{t} \omega_{j,\lambda} \sum_{i=1}^{n} (y_{ij} - \widehat{B}_0 - \widehat{B}_1 x_i^* - \cdots - \widehat{B}_m x_i^{*m})^2.$$

Let $\widehat{\theta}_t = (\widehat{B}_0, \widehat{B}_1, \widehat{B}_2, \cdots, \widehat{B}_m, \widehat{\sigma}_0^2)$, $\theta = (B_0, B_1, B_2, \cdots, B_m, \sigma_0^2)$. Then the $-2\times$logarithm of WLRT statistic can be given as:

$$\begin{aligned} R_{t,\lambda} &= 2\left[Y_t(\widehat{\theta}_t, \lambda) - Y_t(\theta, \lambda)\right] \\ &= 2 \cdot (-\frac{1}{2})\left(Y_{p,t} \log \widehat{\sigma}_0^2 + \widehat{Y}_{c,t}\frac{1}{\widehat{\sigma}_0^2} - Y_{p,t} \log \sigma_0^2 - Y_{c,t}\frac{1}{\sigma_0^2}\right) \\ &= -\left[Y_{p,t} \log\left(\frac{\widehat{Y}_{c,t}}{\sigma_0^2 Y_{p,t}}\right) + Y_{p,t} - \frac{Y_{c,t}}{\sigma_0^2}\right] \\ &= \frac{Y_{c,t}}{\sigma_0^2} - Y_{p,t} + Y_{p,t} \log\left(\frac{\sigma_0^2 Y_{p,t}}{\widehat{Y}_{c,t}}\right) \\ &= \frac{Y_{c,t}}{\sigma_0^2} + n \log\left(\frac{n\sigma_0^2}{\widehat{Y}_{c,t}}\right) - n. \end{aligned}$$

References

[1] Kang L, Albin SL. On-line monitoring when the process yields a linear profile. J Qual Technol. 2000;32(4):418-426.

[2] Mestek O, Pavlik J, Suchanek M. Multivariate control charts: control charts for calibration curves. Fresen J Anal Chem. 1994;350(6):344-351.

[3] Stover FS, Brill RV. Statistical quality control applied to ion chromatography calibrations. J Chromatogr A. 1998;804(1-2):37-43.

[4] Mahmoud MA, Woodall WH. Phase I monitoring of linear profiles with calibration applications. Technometrics. 2004;46(4):380-391.

[5] Woodall WH, Spitzner DJ, Montgomery DC, Gupta S. Using control charts to monitor process and product quality profiles. J Qual Technol. 2004;36(3):309-320.

[6] Wang K, Tsung F. Using profile monitoring techniques for a data-rich environment with huge sample size. Qual Reliab Eng Int. 2005;21(7):677-688.

[7] Kim K, Mahmoud MA, Woodall WH. On the monitoring of linear profiles. J Qual Technol. 2003;35(3):317-328.

[8] Noorossana R, Amiri A, Vaghefi SA, Roghanian E. Monitoring quality characteristics using linear profile. Proc. 3rd Int. Industr. Eng. Conf. Tehran, Iran. 2004.

[9] Healy JD. A note on multivariate CUSUM procedures. Technometrics. 1987;29(4):409-412.

[10] Zou C, Zhang Y, Wang Z. A control chart based on change-point model for monitoring linear profiles. IIE Trans. 2006;38(12):1093-1103.

[11] Mahmoud MA, Parker PA, Woodall WH, Hawkins DM. A change point method for linear profile data. Qual Reliab Eng Int. 2007;23(2):247-268.

[12] Noorossana R, Amiri A. Enhancement of linear profiles monitoring in Phase II. AmirKabir. 2007;18:19-27.

[13] Woodall WH. Current research on profile monitoring. Produc$\widetilde{a}$o. 2007;17(3):420-425.

[14] Ghahyazi ME, Nikai STA, Soleimani P. On the monitoring of linear profiles in multistage processes. Qual Reliab Eng Int. 2014;30(7):1035-1047.

[15] Jensen WA, Brich JB, Woodall WH. Monitoring correlation within linear profiles using mixed models. J Qual Technol. 2008;40(2):167-183.

[16] Noorossana R, Amiri A, Soleimani P. On the monitoring of autocorrelated linear profiles. Commun Stat-Theor M. 2008;37(3):425-442.

[17] Zhang Y, He Z, Zhang C, Woodall WH. Control charts for monitoring linear profiles with within-profile correlation using Gaussian process models. Qual Reliab Eng Int. 2014;30(4):487-501.

[18] Jin J, Shi J. Feature-preserving data compression of stamping tonnage information using wavelets. Technometrics. 1999;41(4):327-339.

[19] Walker E, Wright WP. Comparing curves using additive models. J Qual Technol. 2002;34(1):118-129.

[20] Ding Y, Zeng L, Zhou S. Phase I analysis for monitoring nonlinear profiles in manufacturing processes. J Qual Technol. 2006;38(3):199-216.

[21] Williams JD, Woodall WH, Birch JB. Statistical monitoring of nonlinear product and process quality profiles. Qual Reliab Eng Int. 2007;23(8):925-941.

[22] Zou C, Tsung F, Wang Z. Monitoring general linear profiles using multivariate exponentially weighted moving average schemes. Technometrics. 2007;49(4):395-408.

[23] Eyvazian M, Noorossana R, Saghaei A, Amiri A. Phase II monitoring of multivariate multiple linear regression profiles. Qual Reliab Eng Int. 2011;27(3):281-296.

[24] Khedmati M, Niaki STA. Phase II monitoring of general linear profiles in the presence of between-profile autocorrelation. Qual Reliab Eng Int. 2016;32(2):443-452.

[25] Zhang J, Li Z, Wang Z. Control chart based on likelihood ratio for monitoring linear profiles. Comput Stat Data Anal. 2009;53(4):1440-1448.

[26] Li Z, Wang Z. An exponentially weighted moving average scheme with variable sampling intervals for monitoring linear profiles. Comput Ind Eng. 2010;59(4):630-637.

[27] Noorossana R, Saghaei A, Amiri A. Statistical analysis of profile monitoring. John Wiley & Sons, Inc., Hoboken, New Jersey; 1 edition. 2011.

[28] Xu L, Wang S, Peng Y, Morgan JP, Reynolds MR, Woodall WH. The monitoring of linear profiles with a GLR control chart. J Qual Technol. 2012;44(4):348-362.

[29] Zhang Y, He Z, Zhang M, Wang Q. A score-test-based EWMA control chart for detecting prespecified quadratic changes in linear profiles. Qual Reliab Eng Int. 2016;32(3):921-931.

[30] Awad M. Fault detection of fuel systems using polynomial regression profile monitoring. Qual Reliab Eng Int. 2017;33(4):905-920.

[31] Nie B, Du M. Identifying change-point in polynomial profiles based on data-segmentation. Commun Stat-Simul Comput. 2017;46(4):2513-2528.

[32] Yang W, Zou C, Wang Z. Nonparametric profile monitoring using dynamic probability control limits. Qual Reliab Eng Int. 2017;33(5):1131-1142.

[33] Liu L, Lai X, Zhang J, Tsung F. Online profile monitoring for surgical outcomes using a weighted score test. J Qual Technol. 2018;50(11):88-97.

[34] Kazemzadeh R, Noorossana R, Amiri A. Phase I monitoring of polynomial profiles. Commun Stat-Thero M. 2008;37(10):1671-1686.

[35] Kazemzadeh R, Noorossana R, Amiri A. Monitoring polynomial profiles in quality control applications. Int J Adv Manuf Technol. 2009;42(7-8):703-712.

[36] Zhou Q, Zou C, Wang Z, Jiang W. Likelihood-based EWMA charts for monitoring poisson count data with time-varying sample sizes. J Am Stat Assoc. 2012;107(499):1049-1062.

[37] Qi D, Wang Z, Zi X, Li Z. Phase II monitoring of generalized linear profiles using weighted likelihood ratio charts. Comput Ind Eng. 2016;94:178-187.

[38] Qi D, Li Z, Zi X, Wang Z. Weighted likelihood ratio chart for statistical monitoring of queueing systems. Qual Technol Quant Manage. 2016;14(1):19-30.

[39] Zhang C, Tsung F, Xiang D. Monitoring censored lifetime data with a weighted-likelihood scheme. Nav Res Log. 2016;63(8):631-646.

[40] Song Z, Liu Y, Li Z, Zhang J. A weighted likelihood ratio test-based chart for monitoring process mean and variability. J Stat Comput Simul. 2018;88(2):1-22.

[41] Yang SF, Arnold BC. Monitoring Process Variance Using an ARL-unbiased EWMA-P Control Chart. J Qual Reliab Eng Int. 2016;32(3):1227-1235.

[42] Han D, Tsung F. A reference-free cuscore chart for dynamic mean change detection and a unifed framework for charting performance comparison. J Am Statist Assoc. 2006;101(473):368-386.

[43] Hawkins DM, Zamba KD. Statistical process control for shifts in mean or variance using a changepoint formulation. Technometrics. 2005;47(2):164-173.

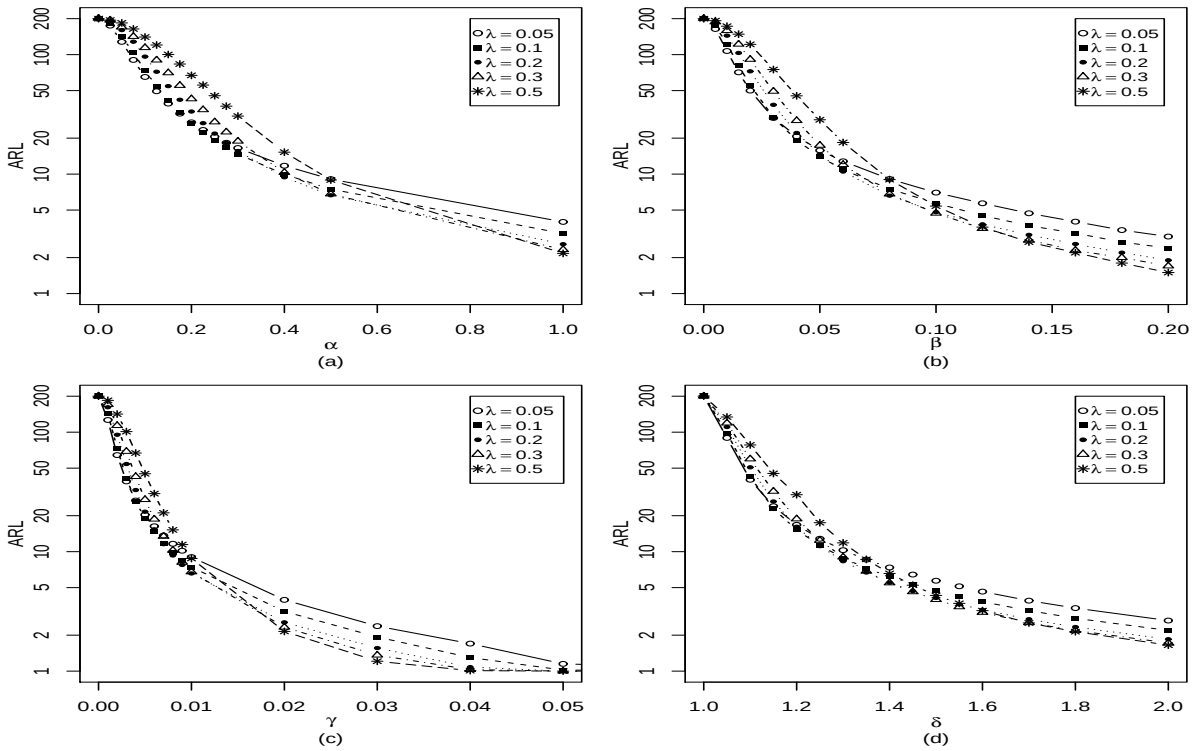

Figure 1: The OC ARL comparisons of the WLRT chart with varying parameters λ

Table 1: The OC ARL comparisons under two terms of A_0, A_1, A_2 shift

	α													
β	0.0	0.025	0.05	0.075	0.1	0.125	0.15	0.175	0.2	0.225	0.25	0.275	0.3	0.4
0.0	199.8	183.7	142.1	103.1	74.7	54.4	41.7	32.7	26.9	22.3	19.1	16.6	14.6	9.9
0.01	123.3	90.4	66.0	49.8	38.3	30.7	25.3	21.3	18.4	16.1	14.3	12.8	11.5	8.4
0.02	56.1	43.1	34.3	28.1	23.4	20.0	17.4	15.4	13.7	12.3	11.2	10.2	9.5	7.2
0.03	29.9	24.8	21.4	18.5	16.3	14.5	13.0	11.8	10.8	10.0	9.2	8.5	8.0	6.3
0.04	19.3	17.1	15.0	13.6	12.3	11.3	10.3	9.5	8.9	8.3	7.8	7.3	6.9	5.6
0.05	14.1	12.7	11.6	10.6	9.9	9.2	8.5	8.0	7.5	7.1	6.7	6.4	6.0	5.0
0.1	5.7	5.4	5.2	5.0	4.8	4.6	4.4	4.3	4.1	4.0	3.8	3.7	3.6	3.2
0.2	2.4	2.3	2.3	2.2	2.2	2.1	2.1	2.1	2.0	2.0	2.0	1.9	1.9	1.8
	α													
γ	0.0	0.025	0.05	0.075	0.1	0.125	0.15	0.175	0.2	0.225	0.25	0.275	0.3	0.4
0.0	200.8	181.9	142.7	103.8	74.7	54.6	41.4	32.6	26.7	22.3	19.0	16.6	14.6	9.9
0.001	141.9	108.6	79.9	59.8	45.2	35.4	28.6	23.8	20.1	17.5	15.3	13.7	12.6	8.8
0.003	40.8	34.1	28.3	24.0	20.6	18.1	16.0	14.3	12.9	11.6	10.6	9.9	9.1	7.0
0.005	18.9	17.0	15.3	13.8	12.6	11.6	10.7	9.9	9.1	8.6	8.0	7.5	7.1	5.7
0.008	9.8	9.2	8.7	8.2	7.8	7.3	6.9	6.6	6.3	6.0	5.7	5.5	5.2	4.4
0.02	3.1	3.0	3.0	2.9	2.8	2.8	2.7	2.6	2.6	2.5	2.5	2.4	2.4	2.2
0.04	1.3	1.2	1.2	1.2	1.2	1.2	1.1	1.1	1.1	1.1	1.1	1.1	1.1	1.0
	β													
γ	0.0	0.005	0.01	0.015	0.02	0.025	0.03	0.035	0.04	0.045	0.05	0.1	0.2	0.3
0.0	200.8	148.8	117.3	96.9	83.7	75.0	68.4	63.7	60.1	57.3	54.9	45.6	41.5	28.4
0.001	133.4	108.0	90.6	79.4	72.0	66.3	62.2	58.8	56.2	53.9	52.0	43.9	40.3	27.5
0.003	80.4	72.2	66.5	62.3	58.9	56.2	54.0	52.0	50.3	48.8	47.4	41.0	37.9	25.9
0.005	62.4	59.0	56.2	54.0	52.0	50.3	48.7	47.3	46.1	44.9	43.9	38.6	35.7	24.2
0.008	51.0	49.4	48.0	46.6	45.4	44.3	43.2	42.3	41.4	40.5	39.6	35.3	32.7	21.8
0.02	33.2	32.5	31.9	31.3	30.8	30.2	29.6	29.0	28.5	27.9	27.4	24.2	22.2	13.8
0.04	16.4	16.0	15.6	15.2	14.9	14.5	14.2	13.9	13.5	13.2	12.9	11.2	10.2	6.8
0.10	3.0	3.0	2.9	2.9	2.9	2.9	2.9	2.9	2.9	2.9	2.8	2.6	2.4	2.0
0.20	1.0	1.0	1.0	1.0	1.0	1.0	1.0	1.0	1.0	1.0	1.0	1.0	1.0	1.0

Table 2: The control limits and corresponding design parameters

Methods	LCL	UCL	design parameters
T^2	—	12.83	—
MCUSUM_1	—	6.25	(3.1,2.025,1.01)
MCUSUM_2	—	6.25	(2.9,1.975,0.99)
χ^2	—	28.2	—
MEWMA	—	0.6711	12.75
Ortho($EWMA_0$)	52.1732	52.8268	3.03
Ortho($EWMA_1$)	6.4431	6.5569	3.03
Ortho($EWMA_2$)	1.9101	2.0899	3.03
Ortho($EWMA_E$)	—	0.5352	3.03
WLRT	—	0.975	—

Table 3: The OC ARL comparisons under shifts in A_0, A_1, A_2, σ_0

	α												
Methods	0.05	0.075	0.10	0.125	0.15	0.175	0.20	0.225	0.25	0.275	0.3	0.4	0.5
MCUSUM/χ^2	136.1	94.1	65.6	47.8	36.1	28.1	23.0	19.2	16.4	14.2	12.6	8.6	6.5
MEWMA	139.5	100.0	70.7	50.6	38.5	29.9	24.3	19.9	17.1	14.8	13.0	8.8	6.7
Ortho	148.7	107.3	74.1	52.3	38.9	29.6	23.7	19.3	16.3	14.1	12.4	8.2	6.2
T^2	189.8	178.2	165.6	149.4	133.7	119.0	103.1	90.6	77.4	67.4	57.4	31.6	17.6
WLRT	141.3	103.8	73.6	54.2	41.6	32.8	26.7	22.4	19.1	16.6	14.7	9.9	7.4
	β												
Methods	0.01	0.02	0.03	0.04	0.05	0.06	0.08	0.10	0.12	0.14	0.16	0.18	0.2
MCUSUM/χ^2	197.4	181.6	162.8	137.9	117.4	100.5	70.7	51.3	38.9	30.2	24.1	19.7	16.6
MEWMA	176.2	127.0	85.6	57.2	40.7	30.6	19.4	13.9	10.8	8.8	7.5	6.5	5.7
Ortho	128.3	57.5	29.8	18.5	13.1	10.3	7.0	5.4	4.4	3.7	3.2	2.8	2.4
T^2	194.3	186.5	172.1	154.3	138.3	119.4	87.3	62.5	44.1	31.3	22.1	16.1	11.8
WLRT	122.7	55.6	29.8	19.2	14.0	10.9	7.5	5.7	4.5	3.7	3.2	2.7	2.4
	γ												
Methods	0.001	0.002	0.003	0.004	0.005	0.006	0.007	0.008	0.009	0.01	0.02	0.03	0.04
MCUSUM/χ^2	197.2	182.8	165.6	145.0	123.4	105.9	89.7	76.6	65.4	57.3	19.6	10.9	7.5
MEWMA	197.8	188.8	170.8	149.0	130.5	112.8	96.7	82.3	71.4	60.8	20.7	11.4	7.8
Ortho	147.7	80.1	44.4	27.9	19.4	14.8	11.8	9.9	8.5	7.5	3.4	1.9	1.2
T^2	198.2	195.6	195.8	190.1	186.8	183.5	178.2	172.3	162.3	159.5	93.4	48.0	24.7
WLRT	142.2	73.6	41.1	26.3	19.0	14.6	11.7	9.8	8.4	7.4	3.1	1.9	1.3
	δ												
Methods	1.05	1.1	1.15	1.2	1.25	1.3	1.35	1.4	1.45	1.5	1.7	1.8	2.0
MCUSUM/χ^2	113.5	65.9	39.1	24.3	16.4	11.2	8.1	6.1	4.8	3.9	2.1	1.7	1.3
MEWMA	95.7	42.3	24.2	16.2	12.1	9.6	8.0	6.8	6.0	5.4	3.8	3.4	2.8
Ortho	71.4	30.4	16.8	11.2	8.3	6.5	5.4	4.6	4.0	3.5	2.4	2.1	1.7
T^2	113.7	71.0	46.3	32.6	23.9	18.1	14.0	11.4	9.4	7.9	4.6	3.7	2.7
WLRT	98.2	42.2	22.8	15.1	11.2	8.8	7.2	6.1	5.3	4.7	3.2	2.7	2.1
	δ												
Methods	0.95	0.90	0.85	0.80	0.75	0.70	0.65	0.60	0.55	0.50	0.45	0.40	0.30
MCUSUM/χ^2	355.6	607.4	971.1	*	*	*	*	*	*	*	*	*	*
MEWMA	174.4	80.0	38.2	22.2	14.9	11.1	6.1	5.3	4.6	4.1	3.7	3.3	2.9
Ortho	465.8	812.5	*	*	*	*	*	*	*	*	*	*	*
T^2	376.9	738.5	*	*	*	*	*	*	*	*	*	*	*
WLRT	124.8	50.4	26.4	17.5	13.2	10.7	9.2	8.1	7.3	6.7	6.3	6.0	5.5

$*$ denotes the corresponding value are larger than 1,000.

Table 4: The OC ARL comparisons under A_0 and A_2 shift simultaneously

Methods	γ	α 0.025	0.05	0.075	0.10	0.125	0.15	0.20	0.25	0.3	0.4
MCUSUM/χ^2	0.001	159.2	115.3	80.4	57.0	42.0	32.2	21.2	15.3	12.0	8.3
MEWMA		167.2	124.9	88.1	62.9	46.0	35.1	22.6	16.2	12.6	8.6
Ortho		112.3	81.4	58.5	43.0	32.6	25.8	17.6	13.0	10.3	7.3
T^2		195.1	186.2	172.2	158.4	143.6	128.5	97.3	73.5	54.8	30.1
WLRT		108.6	79.9	59.8	45.2	35.4	28.6	20.1	15.3	12.6	8.8
MCUSUM/χ^2	0.003	119.0	82.7	58.6	43.6	33.1	26.4	18.1	13.7	10.9	7.8
MEWMA		131.7	95.6	67.7	50.2	37.4	29.5	19.9	14.8	11.7	8.2
Ortho		35.4	28.4	23.2	19.6	16.6	14.4	11.2	9.2	7.7	5.9
T^2		186.9	176.0	162.8	150.4	133.1	116.0	88.3	66.0	49.5	27.3
WLRT		34.1	28.3	24.0	20.6	18.1	16.0	12.9	10.6	9.1	7.0
MCUSUM/χ^2	0.005	86.2	61.2	45.2	34.0	26.9	22.0	15.9	12.4	10.1	7.3
MEWMA		98.3	72.3	52.8	40.0	31.1	25.1	17.6	13.5	10.9	7.8
Ortho		17.0	15.0	13.4	12.0	10.8	9.8	8.3	7.1	6.2	5.0
T^2		175.0	166.8	152.1	136.2	119.9	106.5	80.9	60.3	44.5	24.5
WLRT		17.0	15.3	13.8	12.6	11.6	10.7	9.1	8.0	7.1	5.7
MCUSUM/χ^2	0.01	42.0	32.3	25.8	21.1	17.8	15.4	12.0	9.8	8.4	6.4
MEWMA		47.8	37.2	30.0	24.7	20.7	17.8	13.6	11.0	9.2	6.9
Ortho		7.0	6.7	6.4	6.0	5.7	5.5	5.0	4.5	4.2	3.6
T^2		144.5	131.5	117.8	105.7	92.2	81.4	60.4	45.5	33.2	18.8
WLRT		7.0	6.7	6.4	6.1	5.9	5.6	5.2	4.8	4.4	3.8
MCUSUM/χ^2	0.03	9.9	9.1	8.4	7.8	7.2	6.8	6.0	5.4	4.9	4.2
MEWMA		10.6	9.8	9.2	8.5	8.0	7.6	6.8	6.1	5.6	4.7
Ortho		1.9	1.9	1.8	1.8	1.7	1.7	1.6	1.6	1.5	1.4
T^2		43.0	37.9	33.6	29.8	26.0	22.9	18.1	13.8	11.0	6.9
WLRT		1.9	1.8	1.8	1.8	1.8	1.7	1.7	1.6	1.6	1.5
MCUSUM/χ^2	0.05	5.5	5.2	4.9	4.7	4.5	4.3	4.0	3.7	3.5	3.0
MEWMA		5.8	5.6	5.4	5.2	5.0	4.8	4.5	4.2	4.0	3.6
Ortho		1.0	1.0	1.0	1.0	1.0	1.0	1.0	1.0	1.0	1.0
T^2		12.0	11.0	9.9	8.9	8.1	7.4	6.0	5.0	4.2	3.0
WLRT		1.0	1.0	1.0	1.0	1.0	1.0	1.0	1.0	1.0	1.0

Table 5: The OC ARL comparisons under A_0, A_1 and A_2 shift simultaneously

		γ									
$\alpha = 0.025$	β	0.001	0.002	0.003	0.005	0.008	0.01	0.03	0.05	0.1	0.2
MCUSUM/χ^2	0.005	149.5	129.8	110.2	80.1	50.9	39.2	9.8	5.4	2.4	1.0
MEWMA		163.5	144.8	127.8	96.5	61.8	48.0	10.6	5.8	2.9	1.8
Ortho		74.5	41.9	26.7	14.5	8.4	6.6	1.8	1.0	1.0	1.0
T^2		191.7	189.8	185.8	177.4	158.9	145.6	42.4	12.1	1.7	1.0
WLRT		72.5	40.8	26.4	14.5	8.4	6.5	1.8	1.0	1.0	1.0
MCUSUM/χ^2	0.01	139.8	120.1	102.2	74.2	47.5	37.1	9.6	5.4	2.4	1.0
MEWMA		148.6	134.8	119.7	92.4	60.1	46.3	10.6	5.8	2.9	1.8
Ortho		50.6	30.8	21.2	12.5	7.7	6.2	1.8	1.0	1.0	1.0
T^2		190.3	185.6	184.4	176.3	157.7	144.4	42.1	11.9	1.7	1.0
WLRT		50.1	30.7	21.2	12.8	7.8	6.1	1.8	1.0	1.0	1.0
MCUSUM/χ^2	0.015	128.9	109.8	92.7	79.3	44.4	34.8	9.4	5.3	2.4	1.0
MEWMA		131.5	120.7	107.4	82.9	56.5	44.5	10.5	5.8	2.9	1.8
Ortho		36.2	23.8	17.5	11.0	7.1	5.8	1.8	1.0	1.0	1.0
T^2		187.8	181.5	178.5	170.2	155.3	142.1	42.9	12.1	1.7	1.0
WLRT		35.8	24.1	17.7	11.2	7.2	5.8	1.7	1.0	1.0	1.0
MCUSUM/χ^2	0.03	100.4	85.8	73.3	54.3	36.6	29.4	8.9	5.1	2.3	1.0
MEWMA		77.9	73.9	68.4	57.7	43.4	35.9	10.2	5.8	2.9	1.8
Ortho		17.4	13.7	11.1	8.1	5.8	4.9	1.6	1.0	1.0	1.0
T^2		168.9	167.2	163.1	155.8	139.5	129.4	39.6	11.7	1.7	1.0
WLRT		18.3	14.2	11.5	8.4	5.9	4.9	1.6	1.0	1.0	1.0
MCUSUM/χ^2	0.04	84.9	71.8	62.1	47.3	32.9	26.8	8.6	5.0	2.3	1.0
MEWMA		54.4	52.6	49.5	43.7	35.1	30.4	9.9	5.7	2.9	1.8
Ortho		12.6	10.5	8.9	6.9	5.2	4.5	1.5	1.0	1.0	1.0
T^2		151.8	151.2	147.8	141.8	127.7	117.9	38.4	11.5	1.7	1.0
WLRT		13.4	11.1	9.3	7.1	5.2	4.4	1.6	1.0	1.0	1.0
MCUSUM/χ^2	0.05	72.2	63.3	53.6	41.4	29.2	24.5	8.3	5.0	2.2	1.0
MEWMA		39.5	38.2	37.1	33.6	28.4	25.5	9.6	5.6	2.9	1.8
Ortho		9.9	8.5	7.5	6.0	4.7	4.1	1.5	1.0	1.0	1.0
T^2		134.6	132.4	131.1	124.7	113.1	106.6	35.5	11.0	1.6	1.0
WLRT		10.6	9.0	7.9	6.2	4.7	4.0	1.5	1.0	1.0	1.0

Table 6: The OC ARL comparisons under A_0, A_1, A_2 and σ shift simultaneously

		δ									
$\alpha = 0.025$ $\beta = 0.005$	γ	1.05	1.1	1.15	1.2	1.25	1.3	1.4	1.5	1.7	2.0
MCUSUM/χ^2	0.001	94.1	58.6	36.8	23.7	15.9	11.1	6.1	3.9	2.2	1.4
MEWMA		84.2	40.3	23.6	15.9	12.1	9.6	6.9	5.4	3.9	2.8
Ortho		44.8	25.1	15.5	10.8	8.1	6.4	4.6	3.6	2.5	1.7
T^2		111.9	70.5	46.0	32.4	23.6	18.1	11.3	7.8	4.5	2.7
WLRT		51.3	31.0	19.8	14.0	10.6	8.4	6.0	4.6	3.1	2.1
MCUSUM/χ^2	0.003	76.8	51.1	33.6	22.7	15.5	10.9	6.1	3.9	2.2	1.4
MEWMA		73.6	37.7	22.7	15.6	11.9	9.5	6.9	5.4	3.8	2.8
Ortho		22.4	17.1	12.6	9.5	7.4	6.1	4.5	3.5	2.4	1.7
T^2		106.9	68.1	45.2	31.7	23.3	17.9	11.3	7.8	4.6	2.8
WLRT		23.2	18.5	14.4	11.3	9.2	7.6	5.6	4.4	3.1	2.1
MCUSUM/χ^2	0.005	61.2	44.3	30.7	21.3	14.9	10.8	6.1	3.9	2.2	1.4
MEWMA		60.8	34.3	21.6	15.3	11.8	9.4	6.8	5.3	3.8	2.8
Ortho		13.5	11.7	9.8	7.9	6.7	5.6	4.1	3.3	2.4	1.7
T^2		103.2	66.3	44.2	31.3	22.9	17.3	11.1	7.7	4.5	2.7
WLRT		13.6	12.1	10.4	8.9	7.7	6.6	5.1	4.1	3.0	2.6
MCUSUM/χ^2	0.01	34.4	28.6	22.7	17.3	13.0	9.8	5.8	3.8	2.1	1.4
MEWMA		36.3	25.5	18.4	13.7	10.8	8.9	6.6	5.2	3.8	2.8
Ortho		6.4	6.1	5.7	5.2	4.7	4.2	3.5	2.9	2.2	1.6
T^2		88.2	57.4	39.3	27.6	20.9	16.2	10.5	7.4	4.4	2.8
WLRT		6.3	6.0	5.6	5.3	4.9	4.5	3.9	3.4	2.6	1.9
MCUSUM/χ^2	0.03	9.5	9.2	8.6	7.9	6.9	6.1	4.4	3.2	1.9	1.3
MEWMA		10.2	9.5	8.8	7.9	7.2	6.5	5.4	4.6	3.6	2.7
Ortho		1.8	1.8	1.7	1.7	1.7	1.6	1.5	1.5	1.3	1.2
T^2		30.8	23.2	17.7	14.2	11.7	9.6	7.1	5.4	3.6	2.5
WLRT		1.8	1.8	1.7	1.7	1.7	1.6	1.6	1.5	1.4	1.3
MCUSUM/χ^2	0.05	5.3	5.1	4.9	4.7	4.3	3.9	3.1	2.6	1.8	1.3
MEWMA		5.7	5.6	5.5	5.2	4.9	4.7	4.3	3.9	3.2	2.6
Ortho		1.0	1.0	1.0	1.0	1.0	1.0	1.0	1.0	1.0	1.0
T^2		10.0	8.6	7.4	6.4	5.6	5.0	4.2	3.5	2.8	2.1
WLRT		1.0	1.0	1.0	1.0	1.0	1.0	1.0	1.0	1.0	1.0

Table 7: In control ARL and SDRL comparisons when m Phase I samples are used to estimate the unknown parameters

			k				
λ	UCL		10	30	50	70	100
0.05	0.434	ARL	84.4	124.6	142.1	153.9	167.5
		SDRL	114.7	113.9	139.7	143.3	149.9
0.10	0.975	ARL	103.7	147.5	168.2	179.9	194.6
		SDRL	142.3	164.7	175.2	179.5	189.4
0.20	2.180	ARL	120.8	163.8	181.7	192.7	200.9
		SDRL	119.0	155.1	179.8	189.3	197.1

Table 8: The corrected control limits with estimated parameters (n=10)

	k				
λ	10	30	50	70	100
0.05	0.503	0.470	0.460	0.453	0.448
0.10	1.070	1.015	1.000	0.988	0.980
0.20	2.310	2.230	2.205	2.190	2.180

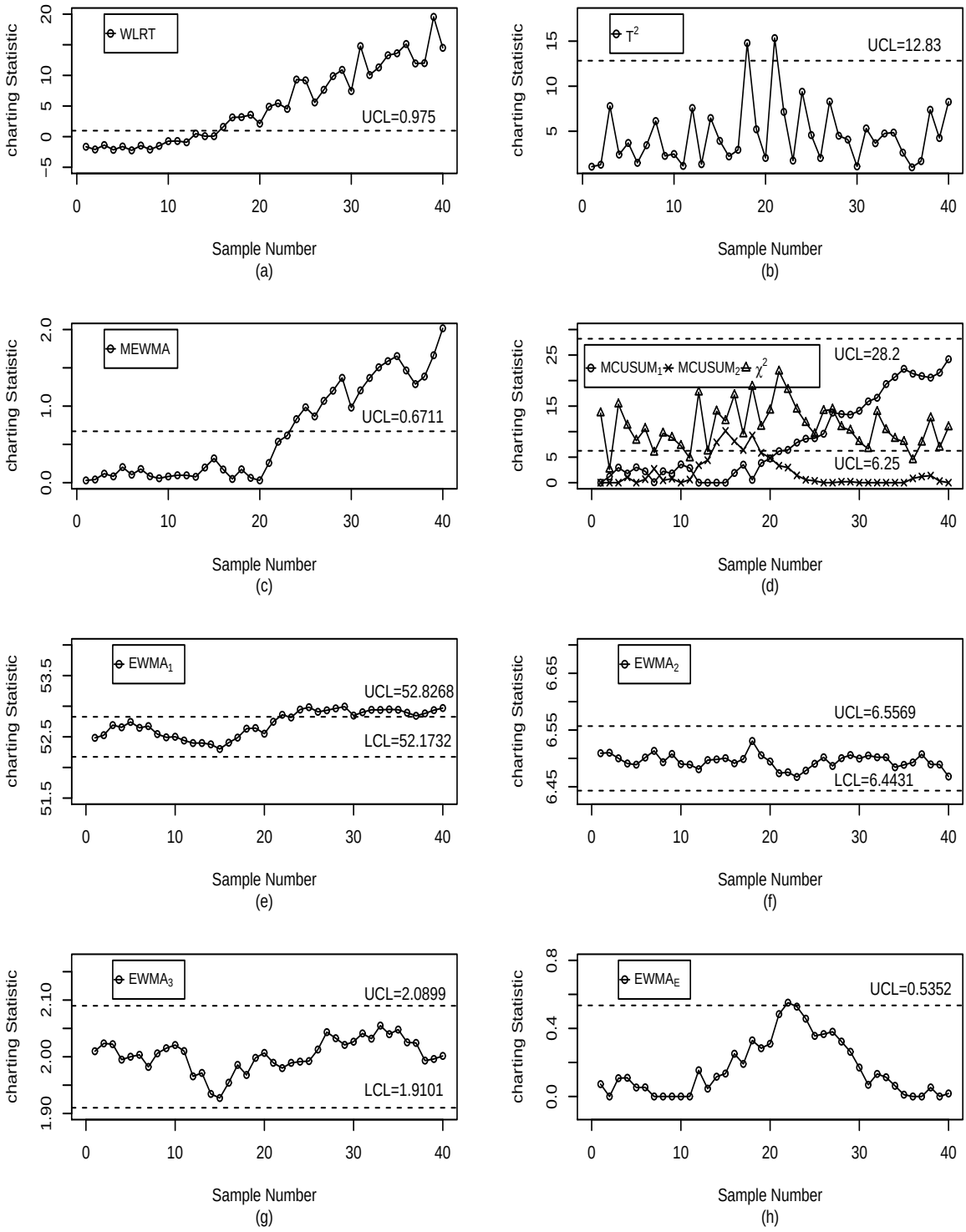

Figure 2: The comparison of control charts for the simulated data